Applied Catalysis B: Environmental 168-169 (2015) 164–174

Contents lists available at ScienceDirect

Applied Catalysis B: Environmental

journal homepage: www.elsevier.com/locate/apcatb

A study on characterization and methane dry reforming performance of Co–Ce/ZrO_2 catalyst

A. Ipek Paksoy[a], Burcu Selen Caglayan[a,b], A. Erhan Aksoylu[a,*]

[a] Department of Chemical Engineering, Bogazici University, 34342 Bebek, İstanbul,Turkey
[b] Advanced Technologies R&D Center, Bogazici University, 34342 Bebek, İstanbul,Turkey

ARTICLE INFO

Article history:
Received 12 August 2014
Received in revised form
18 December 2014
Accepted 21 December 2014
Available online 2 January 2015

Keywords:
Methane dry reforming
CO_2 utilization
Catalytic H_2 production
Non-PGM catalyst

ABSTRACT

The overall purpose of this study is to propose an effective Co-based non-PGM bimetallic carbon dioxide reforming of methane (CDRM) catalyst, and to find the optimal reaction conditions to be used in production of synthesis gas. In catalyst formulation, ZrO_2, which has ability to produce surface oxygen, is used as a support. Ce is used as a promoter in order to increase oxygen storage capacity and to regulate surface oxygen transfer. Freshly reduced and spent catalysts were analyzed by SEM–EDX, HRTEM–EDX, TPO, Raman Spectroscopy and XPS. The reaction conditions were optimised through the use of an experimentally designed procedure using reaction temperature, CH_4/CO_2 feed ratio and space velocity as the parameters. XPS analysis of Co 2p indicated that additional oxidation of Co was limited during CDRM which may only lead to a small decrease in activity. EM measurements showed well dispersion of Co and Ce on the surface. No significant metal sintering was observed. Local changes in Co/Ce ratio were found to have pronounced effect on carbon formation. It is well known that methane dehydrogenation produces surface carbon as the side product covering the active site. The comparative analysis of extent of carbon coverage on Co and Ce sites of the freshly reduced and spent samples through metal mapping by SEM–EDX indirectly confirmed methane dehydrogenation is the primary function of Co sites, and there is no methane activation on Ce sites. A comparative evaluation of XPS Ce 3d obtained from freshly reduced and spent samples on the other hand showed the surface oxygen storage/transfer function of Ce through redox cycle. In the performance tests, high activity with stable performance was observed for $1/1 CH_4/CO_2$ feed ratio for CDRM over Co–Ce/ZrO_2 catalyst.

1. Introduction

Carbon dioxide reforming of methane (CDRM) is a catalytic process that produces valuable synthesis gas from methane and carbon dioxide. Compared to other reforming routes, such as steam reforming (SR) or partial oxidation (POX), CDRM has the advantage of utilizing carbon dioxide, which is the most thermodynamically stable greenhouse gas whose concentration rise in the atmosphere has been accepted as the most plausible reason for the recent climate change. CDRM can be directly used without any pre-separation in producing syngas from natural gas, which may have large amount of CO_2 [1]. The low H_2/CO ratio obtained in CDRM is preferable in production of valuable, especially olefinic, hydrocarbons and alcohols *via* further reactions, like Fischer–Tropsch. Since the reaction is highly endothermic, CDRM can be also used in chemical energy transmission and storage systems [2]. Moreover, the process is suitable to be used in recovering excess heat from gas turbine exhaust, and as a source of CO and H_2 for flame stabilization in low temperature methane fired gas turbines [3].

The main drawbacks of CDRM are coking and metal sintering. Methane decomposition and carbon monoxide disproportionation through Boudouard reaction are possible reasons of coke formation and deposition. The former is favored at high temperatures and low pressures, whereas the latter is favored at low temperatures and high pressures [4]. The high temperature window required for CDRM, and the formation of H_2O by the reversed water gas shift reaction make the catalysts sensitive to metal sintering [5].

Although noble metals exhibit good activity and suffer less from carbon deposition, they have the drawback of high cost and limited availability [6,7]. As they are relatively cheap and possess high activity, industrial nickel-based catalysts have been preferred for reforming reactions. However, at high CDRM temperatures, they deactivate quickly due to metal sintering and coke deposition.

In designing non-noble metal based catalysts, coke resistance and stable performance can be achieved through the use of a suitable metal(s)–support combination leading beneficial synergy between metal and support [8,9]. The carbon formation in CDRM

* Corresponding author. Tel.: +90 212 3597336; fax: +90 212 2872460.
E-mail address: aksoylu@boun.edu.tr (A.E. Aksoylu).

http://dx.doi.org/10.1016/j.apcatb.2014.12.038
0926-3373/

can be controlled by using a support, like ZrO_2, favoring surface oxygen production *via* dissociative adsorption of CO_2; the carbon formed on the active metal centers is cleaned by this surface oxygen [5,10]. ZrO_2 also has high thermal stability and an appreciable ionic conductivity led by its readiness to form defects and surface oxygen vacancies [11]. Additionally, it is mentioned in literature that the use of supports with low concentration of Lewis acid sites and/or that have basic sites, such as ZrO_2, MgO, and La_2O_3, lead to high and stable CDRM performance [12].

In CDRM catalysts, Co is a promising choice as a primary metal owing to its stable performance, abundance and relatively low cost. It has been reported that deactivation of Co based catalysts may be due to metal oxidation under reaction conditions as well as coke deposition. Cobalt oxidation and coke deposition can be avoided through optimizing Co loading, using different supports, promoters and reaction conditions [13,14]. Introducing a second metal(ic) component to form a bimetallic catalyst system also improves the anti-coking property of catalysts [15]. Ceria and ceria-based substrates may enhance the catalytic performance by increasing metal dispersion [9]. It has been previously shown by our group that, owing to its redox properties enabling release and restore of oxygen atoms, Ce is an effective promoter for CDRM catalysts regulating surface oxygen transfer to active metal sites [16,17]. These oxygen species react with methane constituents on the surface of the primary metal, which are formed upon CH_4 disproportionation, resulting in reduced coke formation [5]. Besides, the addition of Zr to CeO_2 increases thermal resistance, redox property and oxygen storage capacity of CeO_2 [18].

The overall purpose of this initial study, which is the first paper of a series, is to propose Co–Ce/ZrO_2 system as an effective Co-based non-PGM CDRM catalyst, and to find the optimal reaction conditions to be used in production of synthesis gas leading high and stable activity. In order to increase the oxygen storage capacity of the catalyst, Ce was used as a promoter. The freshly reduced and spent catalyst samples were characterized by using SEM–EDX, HRTEM–EDX, TPO, Raman Spectroscopy and XPS in order to analyze dispersion of the active phases, oxidation state of Co and Ce, extent of carbon coverage of the active sites and types of the carbon formed on those sites. The reaction conditions are optimized through the use of an experimentally designed procedure using reaction temperature, CH_4/CO_2 feed ratio and space velocity as the parameters.

2. Experimental

2.1. Catalyst preparation and pretreatment

5% Co–2% Ce/ZrO_2 catalyst was prepared for the experiments. Zirconia support was first ground and sieved to 45–60 mesh size, and then calcined at 1073 K for 4 h in muffle furnace for high thermal stability. To obtain Co–Ce/ZrO_2 catalyst, impregnation of aqueous precursor solution of Ce (cerium(III) nitrate hexahydrate) was performed first. The slurry obtained after the impregnation step was dried at 388 K overnight. This was followed by heat treatment at 773 K for 4 h and impregnation of aqueous cobalt(II) nitrate hexahydrate solution. Upon Co impregnation, the slurry was again dried at 388 K overnight. Prior to the performance tests, the catalysts were calcined *in situ* in dry air (30 mL/min) for 4 h at 773 K and subsequently reduced *in situ* in H_2 (50 mL/min) for 2 h at the same temperature.

2.2. Catalyst characterization

SEM, energy dispersive X-Ray (EDX) and HRTEM tests were conducted on freshly reduced (*i.e.*, calcined and reduced) Co–Ce/ZrO_2 catalyst samples in order to elucidate their micro-structural properties. The SEM micrographs of the spent catalyst samples tested under different reaction conditions were also used to observe whether there is a change in metal dispersion and the morphology of the deposited carbon. SEM analyses were conducted by using a Philips XL 30 ESEM–FEG system, having a maximum resolution of 2 nm. The experiments were performed at the Advanced Technologies Research and Development Center of Boğaziçi University. HRTEM analyses were carried out at the Institute of Materials at TUBITAK-MAM by using JEOL 2100 LaB6HRTEM operating at 200 kV.

In order to understand the nature of interaction between the dispersed metal species and the support, fresh and spent Co–Ce/ZrO_2 catalyst samples were analyzed by XPS by using Thermo Scientific K-Alpha X-ray Photoelectron Spectrometer at Advanced Technologies Research and Development Center of Boğaziçi University. All binding energies were referenced to the C1s line. For data analysis, the peak intensities were estimated by calculating the integral of each peak, after subtraction of the S-shaped Shirley-type background, and by fitting the curve to a combination of Lorentzian (30%) and Gaussian (70%) lines.

The coke deposited spent catalyst samples were analyzed by temperature programmed oxidation (TPO) and by Raman spectroscopy. The TPO experiments were performed *via* an Intelligent Gravimetric Analyzer (Hiden Isochema) connected online to a dynamic sampling mass spectrometer (Hiden Analytical) for monitoring the combustion products with the following procedure: (i) The spent catalyst sample (~25 mg) was outgassed at 383 K for one hour and then at 298 K overnight to eliminate humidity and trapped gasses, (ii) The sample was subjected to 50 mL/min flow of 5% O_2–95% He mixture at 1 bar, and then heated to 1023 K with 2 K/min heating rate in order to complete coke oxidation. Results from repeated experiments showed that the TPO profiles were reproducible. Raman spectra of the spent catalysts were obtained by using a Renishaw inVia Raman microscope (Advanced Technologies Research and Development Center of Boğaziçi University) with the following operation parameters: 514 nm 20 mW Ar^+ laser as the excitation source; laser intensity of ~2 mW; 5 s acquisition time; a total of 20 accumulation per spectrum. Before measurements, Raman spectrum was calibrated by using a silicon wafer peak at 520 cm^{-1}. All the samples were analyzed under atmospheric condition without pre-treatment with the de-focusing technique.

2.3. Catalytic performance evaluation

Carbon dioxide reforming of methane was carried out in a fixed-bed down-flow tubular 12 mm ID, 70 cm long quartz microreactor under atmospheric pressure over the Co–Ce/ZrO_2 catalyst to see the effects of temperature, CH_4/CO_2 feed ratio and space velocity. Prior to each reaction test, the catalyst was calcined and reduced *in situ*. The reaction tests were performed at the temperature interval of 873–973 K with CH_4/CO_2 feed ratios of 1/1, 2/1, 1/2 and space velocities of 30,000, 20,000 and 10,000 mL/h g-catalyst. Hewlett Packard HP5890, temperature-controlled and programmable gas chromatograph equipped with a thermal conductivity detector (TCD) and a HayeSep D column was used for analyzing the feed and product streams.

3. Results and discussion

3.1. Characterization of Co–Ce/ZrO_2 catalyst

Freshly reduced catalyst samples were characterized by SEM–EDX and HRTEM aiming to study micro-structural properties of the catalysts and dispersion of Co and Ce.

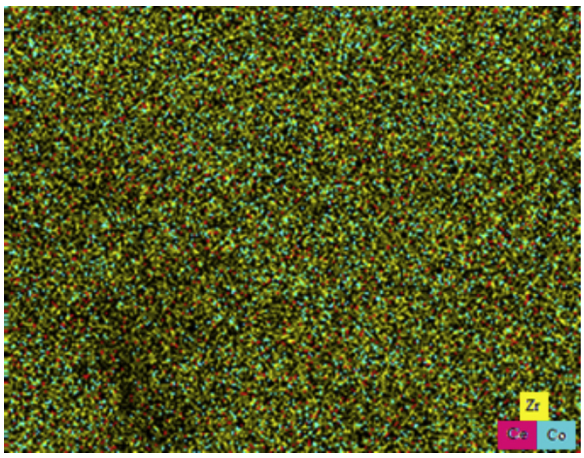

Fig. 1. Co–Ce–Zr mapping of freshly reduced 5% Co–2% Ce/ZrO_2 catalyst.

Table 1
HRTEM-EDX analysis results for the areas in Fig. 2a and b.

Fig. 2	Ce (wt%)	Co (wt%)	Ce/Co	Ce (at%)	Co (at%)	Ce/Co
a	6.57	1.83	3.59	1.23	0.82	1.5
b	5.06	3.24	1.56	1.26	1.92	0.86

The SEM–EDX mapping image (Fig. 1) shows well dispersed metal particles, Co and Ce, on the freshly-reduced catalyst sample. HRTEM results at higher magnifications (Fig. 2), indicated local change in Ce/Co surface ratio. Average Ce/Co surface ratio calculated by using HRTEM–EDX data on different locations of two freshly reduced samples is 1.7, and the highest observed ratio is 3.59. The detailed analysis results of the two selected locations, shown in Fig. 2, are given in Table 1 as examples.

The Ce 3d XP spectrum of the freshly reduced and spent Co–Ce/ZrO_2 catalyst samples were obtained and analyzed aiming to understand the redox ability of CeO_x formations in the freshly reduced sample and how it is changed during the reaction. XP spectra of the spent catalyst samples which were used under reaction conditions yielding the highest, at 973 K with CH_4/CO_2 feed ratio of 2, and the lowest, at 873 K with CH_4/CO_2 feed ratio of 1, coke formation are compared with that obtained from the freshly reduced sample.

The Ce 3d XPS results of the freshly reduced sample are in accordance with the literature (Fig. 3) but peaks are slightly shifted to higher binding energies. There are three main $3d_{5/2}$ peaks at about 887.43 (v), 892.55 (v^2) and 902.69 (v^3) eV and three main $3d_{3/2}$ peaks at about 906.21 (u), 912.5 (u^2) and 919.79 (u^3) eV, which are attributed to the Ce^{4+} state, while the peaks at about 883.01 (v_0), 890.21 (v^1), 904.67 (u_0) and 909.12 (u^1) eV belong to unique photoelectron features of the Ce^{3+} state [19].

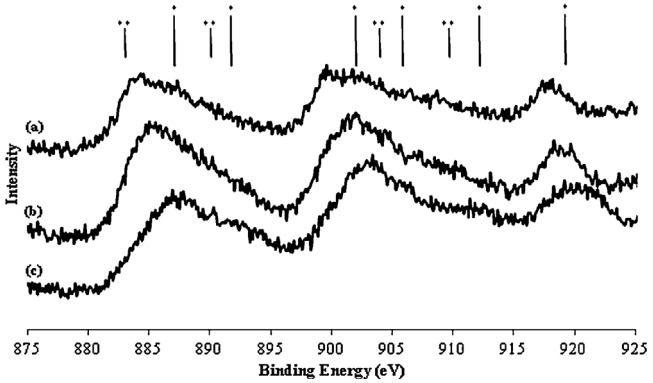

Fig. 3. XP spectrum of Ce 3d region of (a) 5% Co–2% Ce/ZrO_2 catalyst tested at 973 K with 20,000 mL/h g catalyst space velocity and CH_4/CO_2 feed ratio of 2/1, (b) 5% Co–2% Ce/ZrO_2 catalyst tested at 873 K with 20,000 mL/h g catalyst space velocity and CH_4/CO_2 feed ratio of 1/1, and (c) freshly calcined and reduced 5% Co–2% Ce/ZrO_2 catalyst (*: Ce^{4+}, **: Ce^{3+}).

After deconvolution of the spectrum, the degree of ceria reduction was evaluated from the ratio of the sum of integrated peak areas of v_0, u_0, u^1 and v^1 peaks to the sum of the integrated peak areas of all peaks. According to the given equation (Eq. (1)),

$$[Ce^{3+}] = \frac{I - Ce^{3+}}{(I - Ce^{3+} + I - Ce^{4+})} \quad (1)$$

where I-Ce^{3+} and I-Ce^{4+} represent the sum of intensities of two doublets resulting from Ce_2O_3 and three doublets resulting from CeO_2, respectively [19], the amount of Ce^{3+} present on freshly reduced Co–Ce/ZrO_2 catalyst is estimated as 11.6%.

The binding energies attributed to Ce^{4+} and Ce^{3+} states for the spent catalyst samples are given in Table 2. Peaks belonging to both spent catalyst samples were observed to have a shift to lower binding energies when compared to the peaks from the freshly reduced catalyst sample. However, all binding energies found from the deconvolution analysis are in accordance with literature indicating there is no significant possibility of alloy formation [19].

The deconvolution analysis indicated that the degree of ceria reduction is 13.8% for the catalyst tested at 973 K with 2/1 CH_4/CO_2

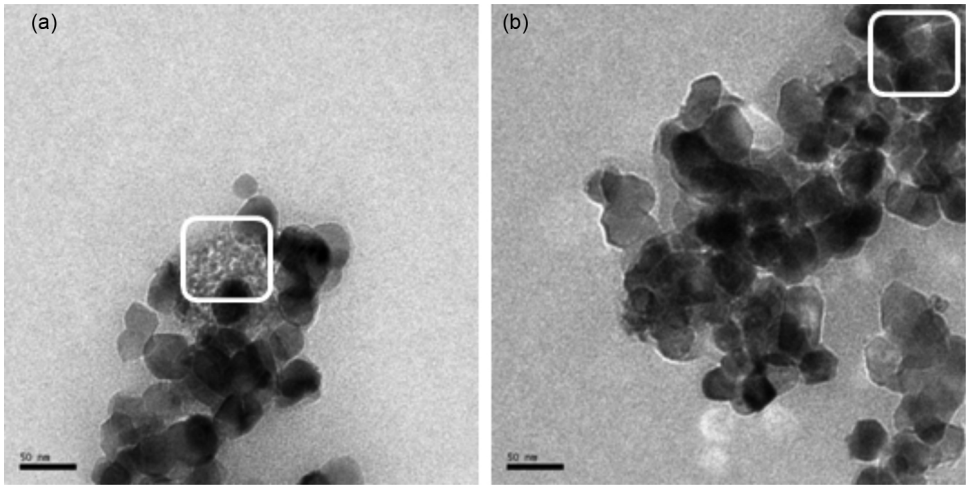

Fig. 2. HRTEM images of selected regions on freshly reduced catalyst sample.

Table 2
The Ce valance-binding energy (eV) relation for different reaction conditions.

Reaction conditions	Ce valance	Binding energy, (eV)
T = 873 K, CH_4/CO_2 = 1/1	Ce^{4+}	919.86, 912.03, 906.63, 902.84, 892.88, 886.88
	Ce^{3+}	909.78, 905.07, 891.02, 882.02
T = 973 K, CH_4/CO_2 = 2/1	Ce^{4+}	918.06, 908.8, 902.69, 899.29, 889.63, 884.01
	Ce^{3+}	905.49, 900.86, 886.72, 880.42

feed ratio, but it is 8.7% for the one tested at 873 K with 1/1 CH_4/CO_2 feed ratio, proving Ce's ability to store oxygen when the feed is rich in oxygen source; *i.e.*, at higher CO_2 concentrations in the feed. This eases the utilization of surface oxygen; during reaction, Ce acts as a buffer regulating surface oxygen transfer from support to Co sites through redox cycle.

Fig. 4 shows the Co 2p XP spectra obtained from freshly reduced and spent catalyst samples. The two peaks, appearing in the spectrum of the freshly reduced sample (Fig. 4c) at 778.8 eV and 793.5 eV, separated by 14.7 eV, may be attributed to the Co $2p_{3/2}$ and Co $2p_{1/2}$ spin–orbit peaks, respectively, of the Co^0 phase, indicating the metallic nature of the reduced catalyst surface. However, as the FWHM of the Co^0 peak is <1.5 eV, in addition to the other deconvoluted peaks corresponding to the main and satellite peaks of the Co^{2+} and Co^{3+} phases, the features attributed to the metal phase are also thought to contain oxide phases [20–23]. The Co 2p XP spectra of both spent catalyst samples informs us about the variation of the Co oxidation state during reaction. The absence of Co^0 $2p_{3/2}$ and $2p_{1/2}$ spin–orbit peaks indicates, in addition to the oxide phases present on the freshly reduced catalyst surface, there is further Co oxide formation during reaction. As can be seen from Fig. 4a and b, the spectra of the spent samples used in reactions conducted at 973 and 873 K, respectively, involve Co $2p_{3/2}$ and Co $2p_{1/2}$ spin–orbit peaks and their satellite features belonging to cobalt oxide phases. It is very difficult to distinguish between the Co^{2+} and Co^{3+} oxide phases due to the small shifts (~0.5 eV) between their peaks. On the other hand, as it has been reported that when Co is deposited onto other oxides the XPS Co 2p lines of Co^{2+} shift to higher BE values, and Co^{2+} has characteristic satellites which are more pronounced in CoO than in Co_3O_4 [20,23], the peaks shown in Fig. 4 are attributed to Co^{2+} phase.

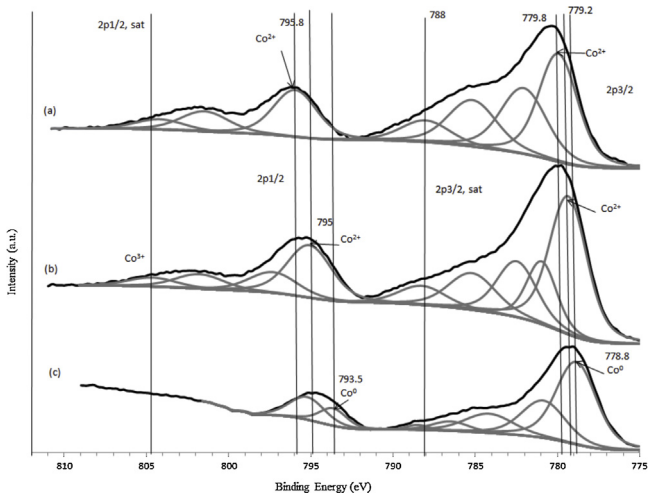

Fig. 4. XP spectrum of Co 2p region of (a) 5% Co–2% Ce/ZrO_2 catalyst tested at 973 K with 20,000 mL/h g catalyst space velocity and CH_4/CO_2 feed ratio of 2/1, (b) 5% Co–2% Ce/ZrO_2 catalyst tested at 873 K with 20,000 mL/h g catalyst space velocity and CH_4/CO_2 feed ratio of 1/1, and (c) freshly calcined and reduced 5% Co–2% Ce/ZrO_2 catalyst.

When the surface metal site is covered even by a thin carbon layer, this site is not seen in metal mapping and the metal's surface concentration, evaluated by EDX, decreases. Considering this fact, a simple methodology, which utilizes a comparative analysis of Co and Ce site concentrations measured on the freshly reduced and spent samples through metal mapping (Fig. 5) and SEM–EDX, was used to investigate the functions of Co and Ce sites in CDRM. The idea behind the methodology is the fact that carbon covers the site whose primary function is hydrogen production from methane/methyl groups, like methane dehydrogenation, forming carbon as the side product. A mild set of CDRM conditions, 873 K with the CH_4/CO_2 feed ratio of 1/1 and space velocity of 20,000 mL/h g catalyst, leading very limited carbon formation was used in preparation of the spent sample. A comparative analysis of EDX results showed that carbon formation is more pronounced on Co sites. The EDX results, on the average, showed that the atomic percentage of Ce is decreased from 0.55 to 0.47 upon 6 h TOS CDRM test, meaning *ca.* 15% of the surface Ce is covered by carbon. On the other hand, under the same conditions, the decrease in Co atomic percentage is from 4.1 to 2.28, meaning *ca.* 44% of Co is covered by carbon. The results clearly showed carbon blockage is significantly more severe on Co centers, confirming the primary function of the Co sites is hydrogen production, whose side product is deposited carbon. The Co and Ce metal mapping images also confirmed this outcome. It should be noted that the carbon covered Ce sites most probably are the ones present in close vicinity of the Co sites on which carbon formed may extend to the neighboring Ce centers.

It is known that the type and amount of coke deposited on the catalyst during CDRM plays an important role in the catalyst performance through affecting its activity and selectivity. In order to understand the effect of local surface Ce concentration on prevention of coke formation, SEM–EDX analyses were performed on spent catalysts used in reaction tests at temperatures of 873 and 973 K, CH_4/CO_2 feed ratios of 1/1 and 2/1 with the space velocity of 20,000 mL/h g catalyst.

Two distinct, namely coked and coke-free, regions observed for each one of the spent Co–Ce catalyst samples, tested under four different reaction conditions, are presented as examples (Fig. 6). EDX analyses (Table 3) performed for both regions on each sample reveal that Ce/Co surface molar ratio of coked parts is lower than that of the coke-free parts. The results confirmed that the presence of ceria on the surface creates an additional storage capacity for oxygen coming from ZrO_2 support, which is known to catalyze CO_2 disintegration generating surface oxygen [24]. Ce centers go through continuous reduction/oxidation cycle during the reaction; they act as a buffer for surface oxygen, regulating and enhancing oxygen transfer to Co centers [17]. This transfer removes deposited carbon through oxidation and makes catalytic centers more carbon resistant. It is observed from the images that formation of carbon is favored for the regions with low Ce/Co ratio. It should be noted that there may be also a possibility of increased Co–Ce interaction.

Many studies have shown that during CDRM, surface oxygen (or oxygen-containing species) originating from CO_2, oxidize carbon species formed by CH_4 decomposition on the metallic sites. Therefore, the rate of carbon accumulation on the catalyst surface is determined by the relative rates of the generation and oxidative removal of carbon species. Excess carbon deposition will occur when the former is faster than the latter [13,20]. SEM analyses (Fig. 7) obtained from the spent samples tested at different temperature and CH_4/CO_2 feed ratios gave information about the relation between reaction conditions, yielding changes in the relative rates of carbon generation and removal, and the type and abundance of carbon deposition.

High level of carbon deposition was observed on the spent sample tested at 973 K with 1/1 CH_4/CO_2 feed ratio, indicating that condition favors carbon formation more than carbon oxidation.

When the CH_4/CO_2 feed ratio was increased to 2/1 while keeping the temperature and space velocity fixed, the highest coke deposition was observed. In addition to the temperature effect, another reason for higher coke accumulation is the higher amount of carbon

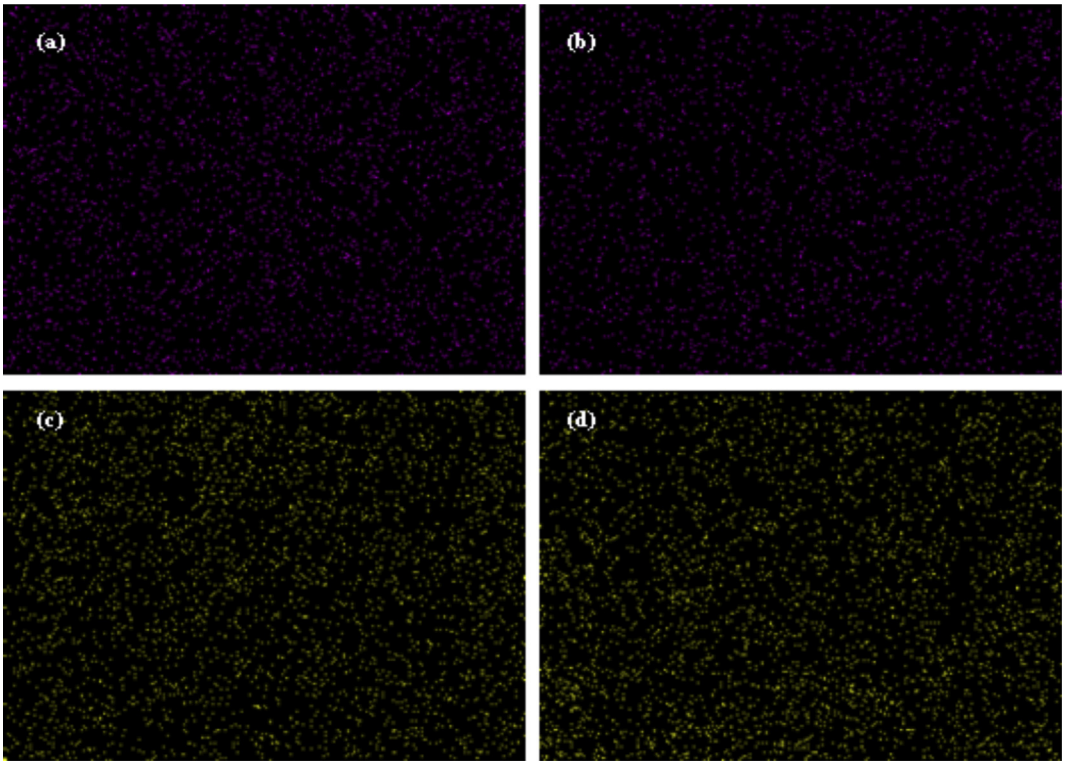

Fig. 5. Co–Ce mapping of 5% Co–2% Ce/ZrO_2 catalyst (a) Co mapping of freshly reduced catalyst, (b) Co mapping of spent catalyst sample used during the reaction performed at 873 K and CH_4/CO_2 = 1/1, (c) Ce mapping of freshly reduced catalyst, (d) Ce mapping of spent catalyst sample used during the reaction performed at 873 K and CH_4/CO_2 = 1/1.

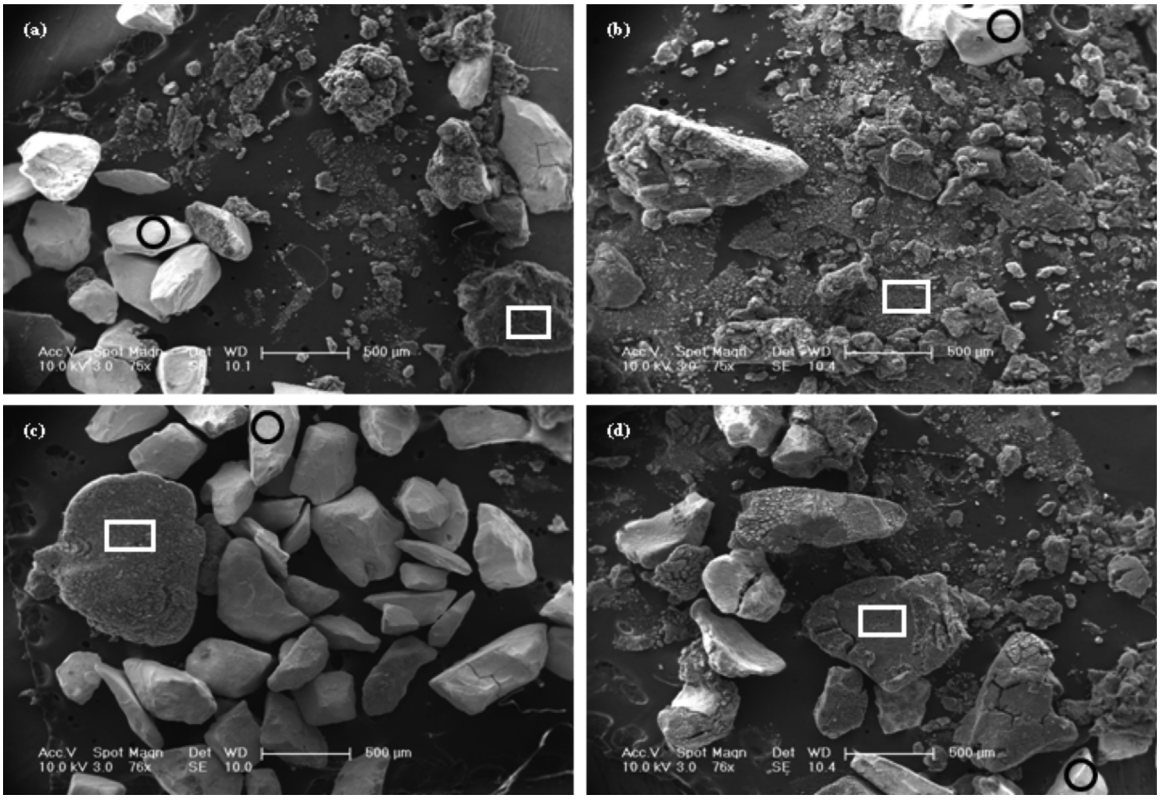

Fig. 6. SEM images of Co–Ce catalyst samples used during the reactions performed at (a) 973 K and CH_4/CO_2 = 1/1, (b) 973 K and CH_4/CO_2 = 2/1, (c) 873 K and CH_4/CO_2 = 1/1, (d) 873 K and CH_4/CO_2 = 2/1 (the regions for which EDX analyses were performed are shown by circles for coke-free regions and by rectangles for coked regions).

Table 3
Ce and Co surface atomic percentages of the spent catalysts obtained by SEM–EDX analysis.

Reaction conditions	Ce (%) coked part	Co (%) coked part	Ce/Co coked part	Ce (%) coke-free part	Co (%) coke-free part	Ce/Co coke-free part
T = 973 K, CH_4/CO_2 = 1/1	0.35	1.25	0.28	1.89	3.10	0.61
T = 973 K, CH_4/CO_2 = 2/1	0.43	0.97	0.44	1.42	3.15	0.45
T = 873 K, CH_4/CO_2 = 1/1	0.56	2.03	0.28	1.39	2.60	0.54
T = 873 K, CH_4/CO_2 = 2/1	0.24	0.89	0.27	1.40	2.79	0.50

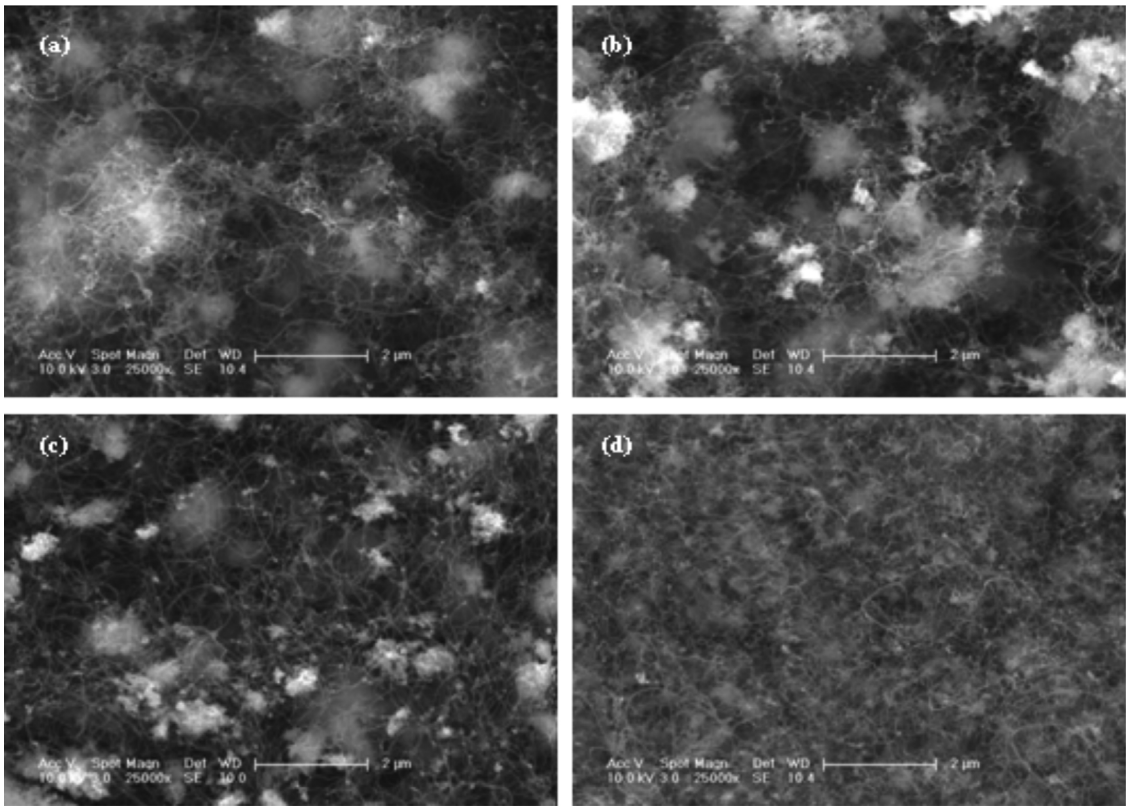

Fig. 7. SEM images of the catalyst samples used during the reaction at space velocity of 20,000 mL/h g-catalyst and at (a) 973 K, CH_4/CO_2 = 1/1 (b) 973 K, CH_4/CO_2 = 2/1 (c) 873 K, CH_4/CO_2 = 1/1 (d) 873 K, CH_4/CO_2 = 2/1.

source in the feed relative to the oxygen source, led by the increased methane concentration in the feed. Consequently, coke deposition is strongly favored when CH_4/CO_2 feed ratio and reaction temperature are both high.

On the other hand, it was seen that coke formation decreased with a decrease in reaction temperature in 873–973 K temperature region. From the SEM image of the sample tested at 873 K, with the CH_4/CO_2 feed ratio of 1/1 and space velocity of 20,000 mL/h g-catalyst, the lowest carbon deposition was observed. It should be noted that Boudouard reaction favored at low temperatures was thought not significant except CDRM tests conducted at 873 K. Although the temperature parameter was still 873 K, the increased, 2/1, ratio of CH_4/CO_2 in the feed caused carbon formation, indicating relatively limited carbon oxidation activity.

The structure of the deposited carbon formed on the spent catalyst samples was further characterized by Raman spectroscopy and temperature programmed oxidation (TPO). The catalyst samples yielding the highest, at 973 K with CH_4/CO_2 feed ratio of 2, and the lowest, at 873 K with CH_4/CO_2 feed ratio of 1, coke formation were chosen for analysis. The Raman spectra of both spent catalyst samples given in Fig. 8 show two well defined bands at around 1344 and 1580 cm^{-1}, which are attributed to the D band, associated with the disordered structural mode of crystalline carbon species, and G band, corresponding to the graphitic carbon with high degree of symmetry, respectively [20,25,26]. The relative intensity of D and G bands (I_D/I_G) gives information about the degree of crystallinity; smaller I_D/I_G value indicates higher crystallinity [20]. The I_D/I_G val-

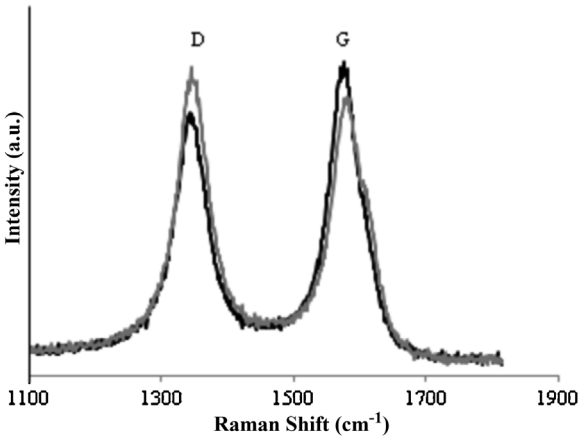

Fig. 8. Raman spectra of the catalyst samples used during the reaction at space velocity of 20,000 mL/h g-catalyst and at (black curve) 973 K, CH_4/CO_2 = 2/1; (grey curve) 873 K, CH_4/CO_2 = 1/1.

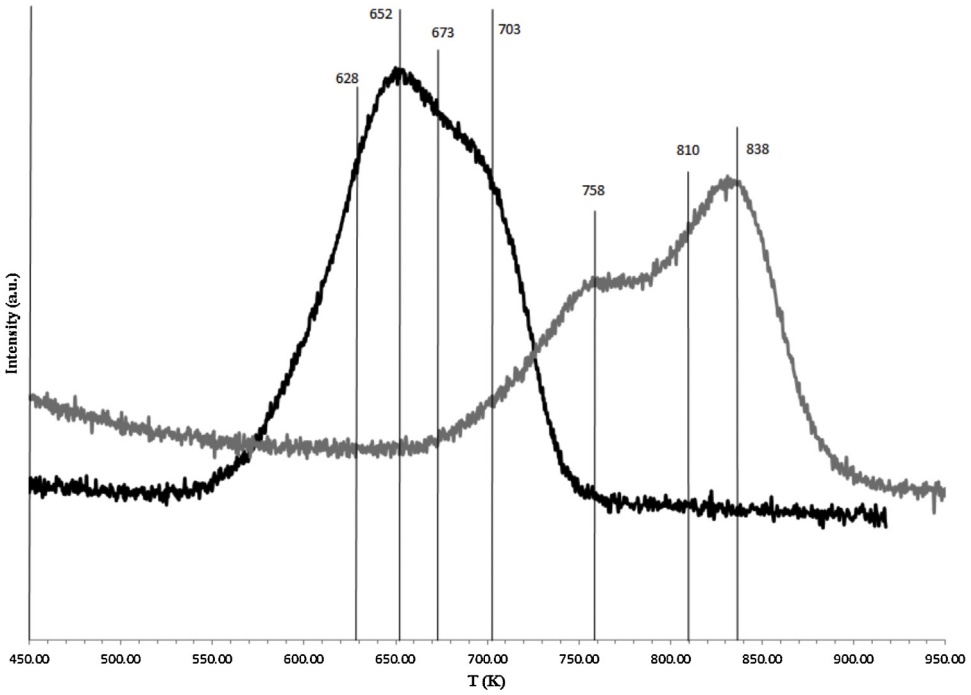

Fig. 9. TPO of the catalyst samples used during the reaction at space velocity of 20,000 mL/h g-catalyst and at (black curve) 973 K, CH_4/CO_2 = 2/1; (grey curve) 873 K, CH_4/CO_2 = 1/1.

ues were calculated as 0.83 and 1.13 for the catalyst samples spent at 873 and 973 K, respectively; pointing out that the coke formed during reaction at 873 K has higher degree of graphitization.

In TPO tests, it is widely accepted that amorphous carbon species are combusted at lower temperatures, *i.e.*, below 773 K, than crystalline ones [20,26–28]. The TPO profile (Fig. 9) of the catalyst tested at 973 K with 2/1 CH_4/CO_2 ratio, reveals a wide and asymmetric peak that begins around 550 K and ends around 750 K. According to the deconvolution results this wide peak encompasses 4 peaks at 628, 652, 673 and 703 K which are all attributed to the amourphous coke. On the other hand, in accordance with the Raman spectroscopy results, the TPO profile of the catalyst used at 873 K records a wider peak between 670 and 900 K, with 3 major peaks at 758, 810 and 838 K. The higher oxidation temperatures of the deposited carbon on that sample indicates an increase in degree of crystallinity in the carbon structure. The peak evolved at 758 K may be attributed to monoatomic coke, and the latter two major peaks may be assigned to filamentous coke with different degree of crystallization, getting closer to pure grafitic structures with the increase in oxidation temperature [27]. Thus, a combined evaluation of SEM images, Raman results and TPO profiles of spent catalyst samples clearly confirms the formation of different carbon structures on the catalyst samples during CDRM, and indicates that the fraction of different carbon types depends on the reaction conditions.

3.2. Performance tests

A parametric CDRM performance study was conducted on Co–Ce/ZrO_2 system considering reaction temperature, CH_4/CO_2 feed ratio and space velocity as the parameters. H_2/CO ratio in the product stream was used as the measure of selectivity. As the syngas fed to Fischer–Tropsch reactor yields valuable olefins when its H_2/CO ratio is close to 1, obtaining H_2/CO ratio in CDRM product closer to 1 is widely accepted advantageous. The activity of the catalyst was studied and discussed in terms of both CH_4 and CO_2 conversions, and H_2 yield achieved.

No severe activity loss was observed during the performed experiments. The CH_4 conversion results of the reaction tests carried at CH_4/CO_2 feed ratio of 2/1, which was expected to cause the highest activity loss due to the higher loading of CH_4, indicated only 25% decrease at most in terms of methane conversion during the time-on-stream (TOS) experiments (Fig. 10). This activity loss was consistent with the carbon deposition observed in SEM analysis (Fig. 7). Main activity loss was observed for the first 15 min TOS for all temperature levels indicating coke formation was more rapid than carbon oxidation reaction on the freshly reduced sample, leading to an activity decrease (Fig. 10). When the rates of methane dehydrogenation and oxidation of carbon formed on Co sites become compatible, the activity level is stabilized. The activity and selectivity profiles indicate that the performance of the catalyst is very stable when the CH_4/CO_2 feed ratio is 1/1 for the whole temperature range except at 873 K, which hints limited carbon removal

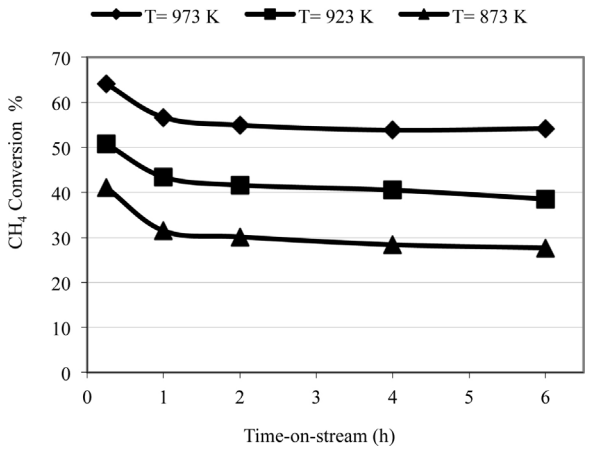

Fig. 10. Time-on-stream activity profiles of the catalyst in terms of CH_4 conversion for CH_4/CO_2 feed ratio of 2/1.

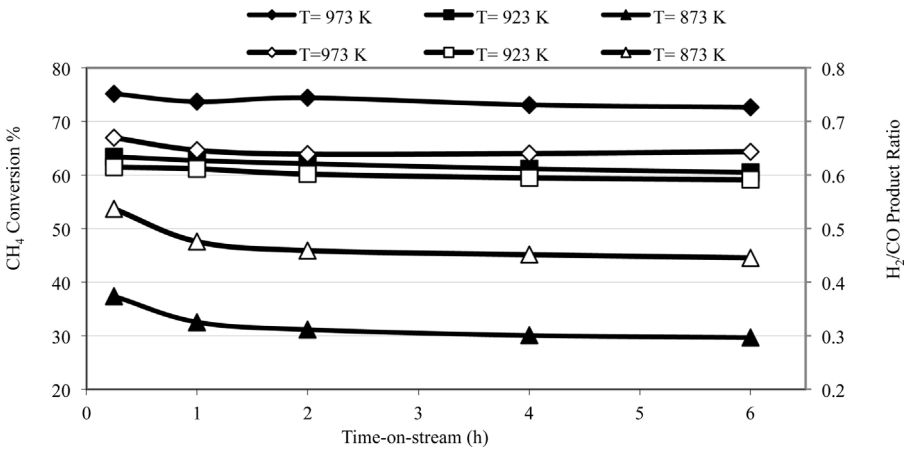

Fig. 11. Time-on-stream activity and selectivity profiles of the catalyst in terms of CH_4 conversion and H_2/CO product ratio, respectively, for CH_4/CO_2 feed ratio of 1/1 (filled symbols: conversion; hollow symbols: selectivity).

ability compared to methane dehydrogenation at low temperatures (Fig. 11).

3.2.1. The effect of reaction temperature

The effect of temperature on catalyst performance was analyzed for the temperature range of 873–973 K in a detailed fashion by using feeds having CH_4/CO_2 ratios of 1/2, 1/1 and 2/1 for 20,000 mL/h g-catalyst space velocity.

The effects of temperature and CH_4/CO_2 feed ratio on CH_4 and CO_2 conversion, CH_4/CO_2 activity ratio and H_2/CO product ratio are shown in Fig. 12a–d based on the performance values obtained at the end of 6 h. TOS. For all cases studied, both CH_4 and CO_2 conversion values (Fig. 12a and b) increased with the increase in temperature. At CH_4/CO_2 feed ratio of 1/1, *e.g.*, methane conversions at the end of 6 h TOS were 30%, 61% and 73% for the reaction temperatures of 873 K, 923 K and 973 K, respectively (Fig. 12a). Carbon dioxide conversions, which were higher than that of methane, were measured as 41%, 70% and 83% at 873 K, 923 K and 973 K, respectively (Fig. 12b). It should be noted that the percentage decline in activity with reaction time was inversely proportional to increase in reaction temperature. Therefore, it can be concluded that surface oxygen generation rate increases sharply relative to carbon formation with an increase in temperature. Additionally,

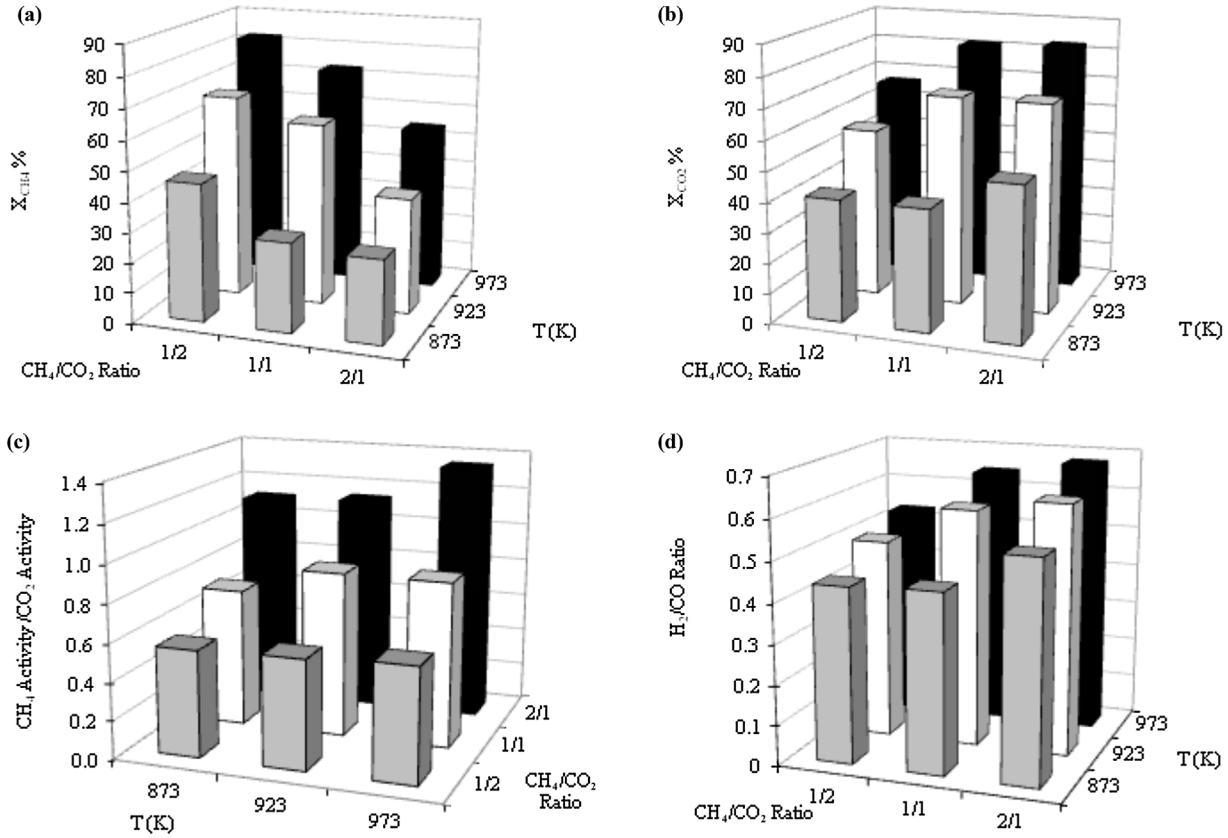

Fig. 12. The effect of reaction temperature and CH_4/CO_2 feed ratio on (a) CH_4 conversion (b) CO_2 conversion (c) CH_4 activity/CO_2 activity ratio (d) H_2/CO product ratio (All values presented were obtained at the end of 6 h. TOS).

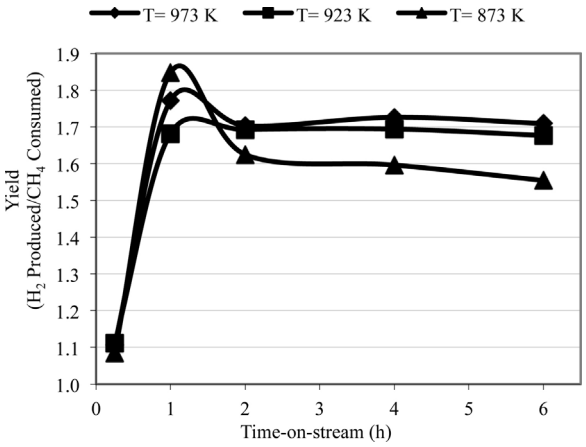

Fig. 13. Time-on-stream profile of H_2 yield (H_2 produced/CH_4 consumed) obtained at CH_4/CO_2 feed ratio of 1/1 and 20,000 mL/h g catalyst.

the activation of surface carbon formed may be more favorable at higher reaction temperatures.

The temperature increase resulted in an increase in the ratio of CH_4 activity to CO_2 activity as the methane decomposition reaction favored at high temperatures (Fig. 12c). The highest observed ratio was 1.35 and it was obtained for the reaction at 973 K with CH_4/CO_2 feed ratio of 2/1. Consequently, both H_2 yield and H_2/CO product ratio (Fig. 12d) increase with the increase in temperature. Stabilized H_2/CO product ratio, at the end of 6 h TOS, was 0.64 at 973 K, 0.59 at 923 K and 0.45 at 873 K for the CH_4/CO_2 feed ratio of 1/1. On the other hand, increase in CH_4 activity relative to that of CO_2 caused higher level of coke deposition which may lead to reactor blockage.

TOS data for H_2 yield (Fig. 13) for the reactions carried out between 873–973 K at CH_4/CO_2 feed ratio of 1/1 reflect the effect of coke deposition. It is evident that coke may form either through methane dehydrogenation or Boudouard reaction. At the beginning of the reaction, surface concentrations of the species are stabilised and the effect of temperature could not be fully observed; as an example, the yield at the end of 1st hour-on-stream was the highest for the test conducted at 873 K. However, with the increase in TOS, Boudouard reaction favored at low temperatures may become relatively significant leading lower H_2 yields at 873 K compared to yields at higher temperatures. The slight increase in "CH_4 activity/CO_2 activity" ratio with temperature (Fig. 12c) supports the dominance of CH_4 dehydrogenation, while relatively higher increase in H_2/CO product ratio with the increase in temperature may indicate the supression of Boudouard reaction at higher temperatures.

Conclusively, it was clearly observed that increasing temperature resulted in increasing activity and selectivity towards hydrogen as well as increasing coke deposition for Ce–Co catalyst in CDRM.

3.2.2. The effect of CH_4/CO_2 feed ratio

The effect of CH_4/CO_2 feed ratio on the activity and selectivity of the Co–Ce catalyst has been studied in a detailed fashion. For the reactions carried out at the same temperature and space velocity, CH_4 activity losses over time were lower at the CH_4/CO_2 feed ratio of 1/2 and 1/1 but significantly high for the feed ratio of 2/1 (Fig. 14). As reaction proceeded, CH_4 conversion decreased by only 3% for the feed ratios of 1/2 and 1/1, whereas the decrease was 15% for the feed ratio of 2/1 at 973 K. The limited activity loss at lower CH_4/CO_2 feed ratios can be attributed to the higher loading of the oxygen source, carbon dioxide. With increased CO_2 feeding rate, carbon formed as the side product of CDRM could be easily cleaned away, resulting in less coke deposition and therefore limited activity loss. This effect is also in agreement with the results of SEM–EDX analysis showing the effect of CH_4/CO_2 feed ratio on deposited carbon (Figs. 6 and 7).

The CH_4/CO_2 feed ratio of 1/2 yielded the highest methane conversion values, whereas the lowest carbon dioxide conversion and H_2/CO product ratio values were obtained for the whole temperature range for that feed ratio (Fig. 12a, b and d). CH_4/CO_2 feed ratio of 2/1, on the other hand, had an opposite effect on catalyst activity and selectivity; it yielded the highest carbon dioxide conversion values and H_2/CO product ratios with the lowest methane conversions observed for the conditions tested. For reactions conducted at 973 K, methane conversion values were 82%, 73% and 54% for the feed ratios of 1/2, 1/1 and 2/1, respectively (Fig. 12a). Carbon dioxide conversion values, on the other hand, were 67% at 1/2 feed ratio, 82% at 1/1 feed ratio and 83% at 2/1 feed ratio (Fig. 12b). At the end of 6-h-on-stream, the highest H_2/CO product ratio, 0.68, was obtained for 2/1 feed ratio whereas the lowest ratio, 0.53, was recorded for the reaction with 1/2 feed ratio (Fig. 12d). It was clearly observed that both conversion and H_2/CO product ratio values were sufficiently high for the tests conducted using 1/1 feed ratio.

When CH_4/CO_2 feed ratio was increased, because of higher loading of hydrocarbon, CH_4 activity increased while CO_2 activity decreased (Fig. 14), leading to an increase in CH_4/CO_2 activity ratio (see Fig. 12c). Considering also the increase in H_2 yield, based on CH_4 fed (not shown), one can explain the enhanced H_2 selectivity in the product stream. However, the increase in CH_4/CO_2 activity ratio caused coke deposition, as there was not enough oxygen source to

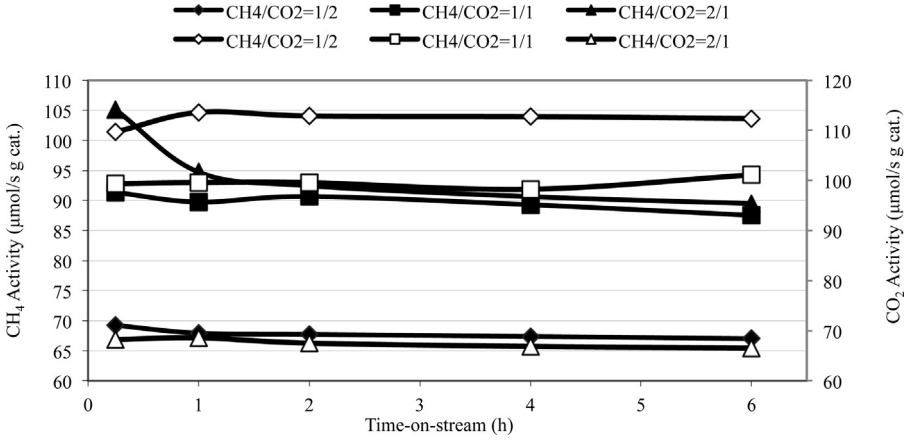

Fig. 14. CH_4 and CO_2 activities at 973 K for 20,000 mL/h g catalyst (filled symbols: CH_4 activity; hollow symbols: CO_2 activity).

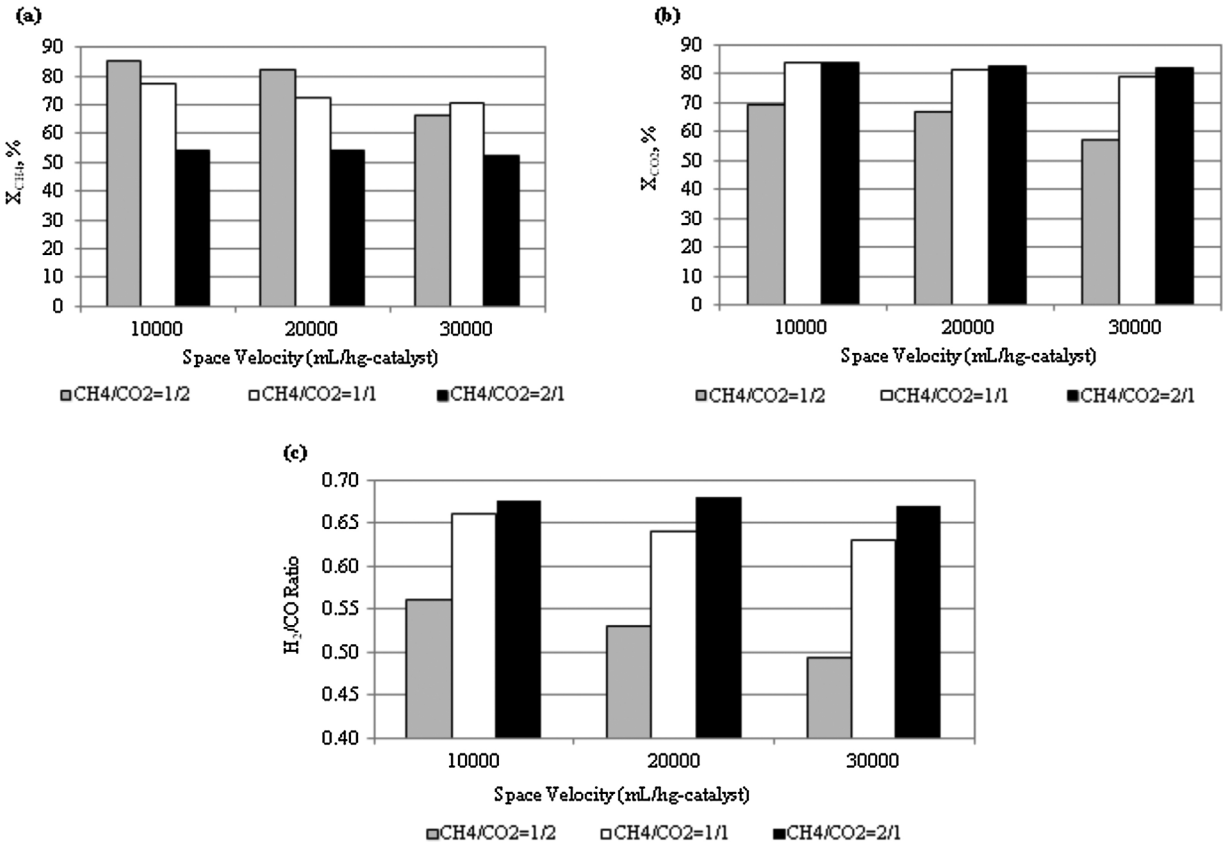

Fig. 15. Activity and selectivity trends at 973 K as a function of CH_4/CO_2 feed ratios and space velocities (a) CH_4 conversions (b) CO_2 conversions (c) H_2/CO product ratio.

clean away the formed carbon and, therefore, H_2 yield, based on CH_4 consumed, was decreased.

It was clear that CH_4/CO_2 feeding ratio has a serious effect on both activity and selectivity of the Ce–Co catalyst. Evaluating activities and coke deposition in a combined fashion indicates that 1/1 feed ratio can be taken as a suitable value for the current catalyst.

3.2.3. *The effect of space velocity*

The effect of space velocity on the CDRM performance of Co–Ce system was investigated for three different space velocities, 10,000 mL/h g-catalyst, 20,000 mL/h g-catalyst and 30,000 mL/h g-catalyst at 973 K for CH_4/CO_2 feed ratio values between 0.5 and 2 (Fig. 15). Similar activity trends were observed for all space velocities tested (not shown).

As the space velocity increased from 10,000 mL/h g-catalyst to 30,000 mL/h g-catalyst, both CH_4 and CO_2 conversion values decreased for all feed compositions (Fig. 15a and b). The decrease was 5% for the CH_4/CO_2 feed ratio of 1/1 and most of the decrease was observed when the space velocity was changed from 10,000 to 20,000 mL/h g-catalyst. At the end of 6th h-on-stream, methane conversions for the feed ratio of 1/1 were recorded as 78%, 73% and 71% for the space velocities of 10,000, 20,000 and 30,000 mL/h g-catalyst, respectively.

It was interesting to notice that the effect of space velocity was observed more significantly as the CH_4/CO_2 feed ratio was decreased. This can be explained by the comparative analysis of methane dehydrogenation and surface carbon oxidation rates. The increase in oxygen source resulted in closer oxidation and dissociation rates leading stable CDRM activity.

There were no major changes observed for H_2/CO product ratio for the CH_4/CO_2 feed ratios of 1/1 and 2/1 in response to changes in space velocity (Fig. 15c). As the space velocity was increased from 10,000 to 30,000 mL/h g-catalyst, H_2/CO product ratio only decreased from 0.66 to 0.64 and 0.68 to 0.67 for CH_4/CO_2 feed ratios of 1/1 and 2/1, respectively. However, H_2/CO product ratio became 0.49 for CH_4/CO_2 feed ratio of 1/2 at 30,000 mL/h g-catalyst, which was 0.56 at 10,000 mL/h g-catalyst.

Based on the results of the experiments carried out, the increase in space velocity resulted in a decrease in both CH_4 and CO_2 conversions and H_2/CO product ratio for all CH_4/CO_2 feed ratios applied.

3.2.4. *Stability Test*

The 72 h stability test was performed over 5% Co–2% Ce–ZrO_2 at 873 K with the CH_4/CO_2 feed ratio of 1/1 and space velocity of 20,000 mL/h g catalyst. Despite very limited coke formation, which was characterized by TPO and Raman analysis, the catalyst showed no deactivation (Fig. 16) during 72-h-on-stream.

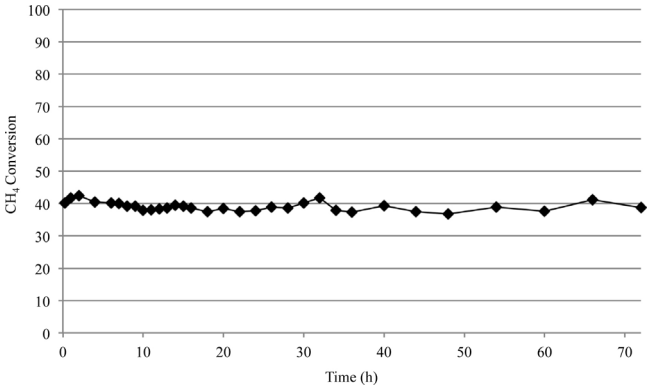

Fig. 16. Stability test over 5% Co–2% Ce/ZrO_2 (873 K, CH_4/CO_2 = 1/1, space velocity = 20000 mL/h g catalyst).

4. Conclusions

Co–Ce/ZrO_2 catalyst was characterized and tested in CDRM for different reaction conditions. The following conclusions can be drawn according to the characterization and catalytic performance data:

- The comparative analysis of Co and Ce site concentrations measured on the freshly reduced and spent samples through metal mapping and SEM–EDX indirectly confirmed that methane dehydrogenation is the primary function of Co sites.
- Combined evaluation of SEM images, Raman results and TPO profiles of spent catalyst samples clearly showed the formation of different carbon structures on the catalyst samples during CDRM, and indicated that the fraction of different carbon types depends on the reaction conditions.
- XPS Ce 3d results revealed that ceria creates an additional oxygen storage capacity resulting in an enhanced surface oxygen storage/transfer function through redox cycle and higher carbon resistance.
- Co–Ce/ZrO_2 catalyst has stable activity for CH_4/CO_2 feed ratio of 1. Coke accumulation was mostly observed when temperature and CH_4/CO_2 feed ratio were both high. Decreasing space velocity is beneficial for high and stable activities and high H_2/CO product ratio.

Acknowledgements

This work is financially supported by TUBITAK through project 111M144, Boğaziçi University through project BAP-M6755, and by State Planning Organization of Turkey through project DPT 07K120630.

References

[1] D. Cheng, X. Zhu, Y. Ben, F. He, L. Cui, C. Liu, Catal. Today 115 (2006) 205–210.
[2] G.S. Gallego, C. Batiot-Dupeyrat, J. Barrault, E. Florez, F. Mondragon, Appl. Catal. A: Gen. 334 (2008) 251–258.
[3] L.A. Arkatova, Catal. Today 157 (2010) 170–176.
[4] G.S. Gallego, F. Mondragon, J. Tatibouet, J. Barrault, C. Batiot-Dupeyrat, Catal. Today 133–135 (2008) 200–209.
[5] S. Corthals, J. Van Nederkassel, J. Geboers, H. De Winne, J. Van Noyen, B. Moens, B. Sels, P. Jacobs, Catal. Today 138 (2008) 28–32.
[6] Z. Hou, P. Chen, H. Fang, X. Zheng, T. Yashima, Int. J. Hydrogen Energy 31 (2006) 555–561.
[7] D. Liu, W.N.E. Cheo, Y.W.Y. Lim, A. Borgna, R. Lau, Y. Yang, Catal. Today 154 (2010) 229–236.
[8] R. Bouarab, O. Akdim, A. Auroux, O. Cherifi, C. Mirodatos, Appl. Catal. A: Gen. 264 (2004) 161–168.
[9] S. Damyanova, B. Pawelec, K. Arishtirova, M.V. Martinez Huerta, J.L.G. Fierro, Appl. Catal. B: Environ. 89 (2009) 149–159.
[10] A.D. Ballarini, S.R. de Miguel, E.L. Jablonski, O.A. Scelza, A.A. Castro, Catal. Today 107–108 (2005) 481–486.
[11] J.D.A. Bellido, E.M. Assaf, Appl. Catal. A: Gen. 352 (2009) 179–187.
[12] M. Rezaei, S.M. Alavi, S. Sahebdelfar, Z. Yan, Scr. Mater. 61 (2009) 173–176.
[13] E. Ruckenstein, H.Y. Wang, J. Catal. 205 (2002) 289–293.
[14] D. San-Joseí Alonso, J. Juan-Juan, M.J. Illan-Gomez, C. Roman-Martinez, Appl. Catal. A: Gen. 371 (2009) 54–59.
[15] J. Xu, W. Zhou, Z. Li, J. Wang, J. Ma, Int. J. Hydrogen Energy 34 (2009) 6646–6654.
[16] S. Ozkara-Aydınoglu, E. Ozensoy, A.E. Aksoylu, Int. J. Hydrogen Energy 34 (2009) 9711–9722.
[17] S. Ozkara-Aydınoglu, A.E. Aksoylu, Catal. Commun. 11 (2009) 1165–1170.
[18] L.V. Mattos, E. Rodino, D.E. Resasco, F.B. Passos, F.B. Noronha, Fuel Process. Technol. 83 (2003) 147–161.
[19] P. Leppet, B. Schumacher, V. Plzak, M. Kinne, R.J. Behm, J. Catal. 244 (2006) 137–152.
[20] M. Dominguez, E. Taboada, H. Idriss, E. Molins, J. Llorca, J. Mater. Chem. 20 (2010) 4875–4883.
[21] J.W. Chai, J.S. Pan, S.J. Wang, C.H.A. Huan, G.S. Lau, Y.B. Zheng, S. Xu, Surf. Sci. 589 (2005) 32–41.
[22] S.S.Y. Lin, D.H. Kim, M.H. Engelhard, S.Y. Ha, J. Catal. 273 (2010) 229–235.
[23] R. Watanabe, Y. Hondo, K. Mukawa, C. Fukuhara, E. Kikuchi, Y. Sekine, J. Mol. Catal. A: Chem. 377 (2013) 74–84.
[24] S. Wang, G.Q. Lu, Appl. Catal. B: Environ. 19 (1998) 267–277.
[25] D.S. Wragg, A. Gronvold, P. Norby, H. Fjellvag, Microporous Mesoporous Mater. 173 (2013) 166–174.
[26] F.F. de Sousa, H.S.A. de Sousa, A.C. Oliveira, M.C.C. Junioe, A.P. Ayala, E.B. Barros, B.C. Viana, J.M. Filho, A.A. Oliveira, Int. J. Hydrogen Energy 37 (2012) 3201–3212.
[27] J. Vicente, J. Erena, C. Montero, M.J. Azkoiti, J. Bilnoa, A.G. Gayubo, Int. J. Hydrogen Energy 39 (2014) 18820–18834.
[28] C.E. Daza, A. Kiennemann, S. Moreno, R. Molina, Appl. Catal. A: Gen. 364 (2009) 65–74.